

Eindhoven University of Technology
Department of Mechanical Engineering
Dynamics and Control Group
P.O.Box 513, 5600 MB, Eindhoven, The Netherlands
E-mail: N.v.d.Wouw@tue.nl

Experimental Facilities

In this report, four experimental systems are described along with the corresponding models which all exhibit non-smooth and/or discontinuous components. In section 1 a drill-string system is described, in section 2 and DVD-ROM drive with an auto-balancing unit is described, in section 3 a controlled robot with friction is discussed and in section 4 an elastic beam with a one-sided support is presented. For each of these systems, the open research questions are posed.

1 Friction-Induced Limit Cycling in an Experimental Drill-String System

Nenad Mihajlovic, Nathan van de Wouw and Henk Nijmeijer
Eindhoven University of Technology
Department of Mechanical Engineering
Dynamics and Control Group

1.1 Introduction

Deep wells for the exploration and production of oil and gas are drilled with a rotary drilling system. A rotary drilling system creates a borehole by means of a rock-cutting tool, called a bit. The torque driving the bit is generated at the surface by a motor with a mechanical transmission box. Via the transmission, the motor drives the rotary table: a large disc that acts as a kinetic energy storage unit. The medium to transport the energy from the surface to the bit is a drill-string, mainly consisting of drill pipes. The lowest part of the drill-string is the Bottom-Hole-Assembly consisting of drill collars and the bit. The drill-string undergoes various types of vibrations during drilling:

- torsional (rotational) vibrations, caused by interaction between the bit and well;
- bending (lateral) vibrations, caused by pipe eccentricity;
- axial (longitudinal) vibrations, due to bouncing of the bit;
- hydraulic vibrations in the circulation system, stemming from pump pulsations.

Drill-string vibrations are an important cause for premature failure of drill-string components and drilling inefficiency. Therefore, an investigation of those vibrations is of interest. In the research which is performed at the Dynamics and Control group of the Mechanical Engineering Department of the Eindhoven University of Technology, torsional drill-string vibrations are investigated. Since the behaviour of the system when a constant torque is applied at the rotary table of a drill-string system is of interest, the focus is on the steady-state behaviour of drill-string systems for such constant torques.

Extensive research on the subject of torsional vibrations has already been conducted [1; 2; 3; 4; 5] According to some of those results, the cause for torsional vibrations is the stick-slip phenomenon due to the friction force between the bit and the well [3; 4; 5]. Moreover, the cause for torsional vibrations can be the negative damping in the friction force present due to the contact between the bit and the borehole, see for example [1; 2]. In order to gain an improved understanding of the causes for torsional vibrations, an experimental drill-string set-up is built. In this set-up, torsional vibrations with and without stick-slip are observed.

1.2 Drill-String Set-Up

The experimental drill-string set-up is shown in Fig. 1. The set-up consists of a power amplifier, a DC-motor, two rotational discs (upper and lower), a low-stiffness string and an additional brake applied to the lower disc. The input voltage from the computer is fed into the DC-motor via the power amplifier. The DC-motor, which represents the drive motor of a real drill rig, is connected, via the gear box, to the upper steel disc (which represents the rotary table of the rig). The upper and lower disc are connected through a low stiffness steel string. The drill-string and the lower brass disc represent the drill-string with the Bottom-Hole-Assembly at the real drill-rig and the additional brake represents the friction force between the drill bit and borehole. The angular positions of the upper and lower disc are measured using incremental encoders. In Fig. 1, θ_u and θ_l are the angular positions of the upper and lower disc, respectively, T_{fru} is the friction torque present at the upper disc and T_{frl} represents the friction torque at the lower disc.

The drill-string set-up is an electro-mechanical system which can be described by:

$$\begin{aligned} J_u \ddot{\theta}_u + k_\theta(\theta_u - \theta_l) + T_{fru}(\dot{\theta}_u) &= k_m u \\ J_l \ddot{\theta}_l - k_\theta(\theta_u - \theta_l) + T_{frl}(\dot{\theta}_l) &= 0, \end{aligned} \tag{1}$$

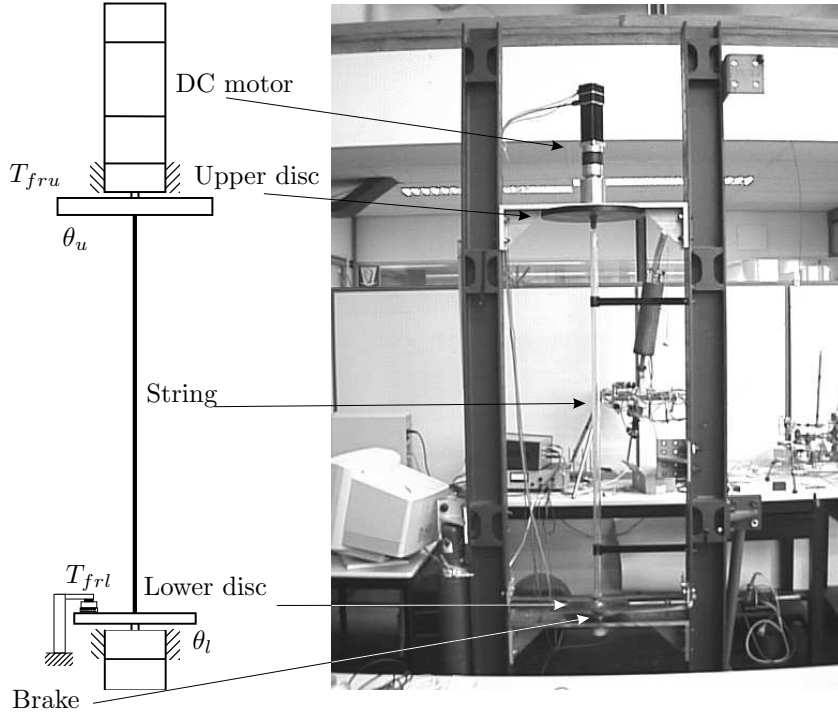


Figure 1: Experimental drill-string set-up.

with the set-valued friction laws

$$\begin{aligned}
 T_{fru}(\dot{\theta}_u) \in \begin{cases} T_{slipup}(\dot{\theta}_u) & \text{for } \dot{\theta}_u > 0, \\ [-T_{slipun}(0), T_{slipup}(0)] & \text{for } \dot{\theta}_u = 0, \\ -T_{slipun}(\dot{\theta}_u) & \text{for } \dot{\theta}_u < 0, \end{cases} \\
 T_{frl}(\dot{\theta}_l) \in \begin{cases} T_{sliplp}(\dot{\theta}_l) & \text{for } \dot{\theta}_l > 0, \\ [-T_{slipln}(0), T_{sliplp}(0)] & \text{for } \dot{\theta}_l = 0, \\ -T_{slipln}(\dot{\theta}_l) & \text{for } \dot{\theta}_l < 0. \end{cases}
 \end{aligned} \tag{2}$$

Therefore, the model of the system, represented by (1) and (2) constitutes a differential inclusion. In (1), J_u and J_l are moments of inertia of the upper and lower disc with respect to the corresponding centres of mass, respectively, u is the input voltage to the power amplifier, k_m represents the motor constant, k_θ is the torsional stiffness of the string. Equation (2) reflects that set-valued friction laws are used to model the friction at the upper and lower disc. The reason for this choice is the fact that in both upper and lower disc, the stick phenomenon is observed. The friction torque at the upper disc T_{fru} is caused by the friction in the gear box, the friction in the bearings at the upper part of the set-up and due to electro-mechanic coupling between rotor and stator of the motor. The friction torque T_{frl} , present at the lower disc, is caused by the friction between lower disc and the brake and the friction in the bearings at the lower disc. Nonlinear functions $T_{slipmp}(\dot{\theta}_u)$, $T_{slipmn}(\dot{\theta}_u)$, $T_{sliplp}(\dot{\theta}_l)$ and $T_{slipln}(\dot{\theta}_l)$ represent complete friction torques which act on the upper and lower disc for nonzero angular velocities and for those nonlinear functions the following conditions hold:

$$\begin{aligned}
 T_{slipup}(\dot{\theta}_u), T_{sliplp}(\dot{\theta}_l) > 0, \forall \dot{\theta}_u, \dot{\theta}_l \geq 0, \text{ and} \\
 T_{slipun}(\dot{\theta}_u), T_{slipln}(\dot{\theta}_l) > 0, \forall \dot{\theta}_u, \dot{\theta}_l \leq 0,
 \end{aligned} \tag{3}$$

which means that the friction torques are dissipative.

1.3 Research questions

In the described set-up the following topics can be interesting for an investigation (see [6]):

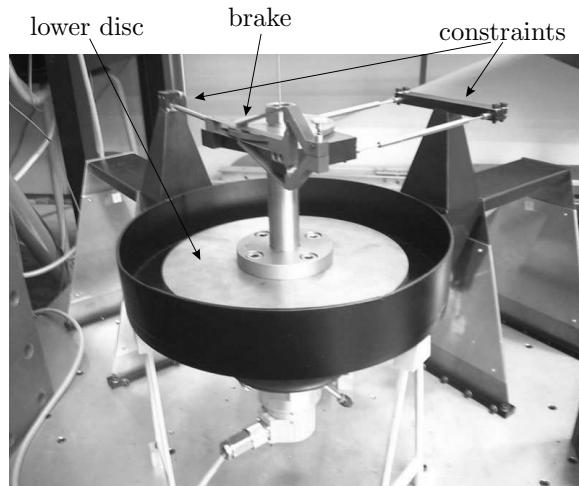
- Experimental investigation of steady-state behaviour for constant inputs (bifurcation analysis),
- Friction modelling,
- Investigation of the effect of different friction situations on the steady-state behaviour,
- Stability of equilibrium sets,
- Bifurcations of equilibria and limit cycles in discontinuous systems.

1.4 Open problems

The aim of future research is not only to gain understanding on torsional vibrations but also the causes for other types of vibrations which appear in the real-life drill-string systems. For this purpose, a new set-up is designed (see Fig. 2). In the new set-up, the lower disc can rotate, but also move in a lateral direction. In order to avoid tilting of the lower disc, additional mechanical constraints are designed. Moreover, a brake is present at the lower part of the set-up which gives the possibility for applying different normal forces at the lower disc leading to different friction forces. With such set-up it is possible to study torsional vibrations and bending vibrations caused by mass unbalancing separately, but also the possible interaction between those two. Moreover, it is possible to add a liquid and therefore to change the viscous friction both in torsional and in lateral direction which is present at the lower disc.



(a) The set-up.



(b) The lower part of the set-up.

Figure 2: Experimental set-up for the investigation of both torsional and bending vibrations.

2 Auto-Balancing Unit

Nathan van de Wouw and Henk Nijmeijer
Eindhoven University of Technology
Department of Mechanical Engineering
Dynamics and Control Group

2.1 Introduction

In machines with rotating components, imbalance is one of the main engineering problems since it causes unwanted vibrations. One solution to this problem is the application of an auto-balancing unit. In principle, an auto-balancing unit is capable of counteracting the imbalance, even when it is a priori unknown. An example of an industrial application in which an automatic balancing unit is implemented is a DVD-player, see figure 3. In this figure, part of a CDROM player is shown, with the optical lens and the auto-balancing unit (ABU). The

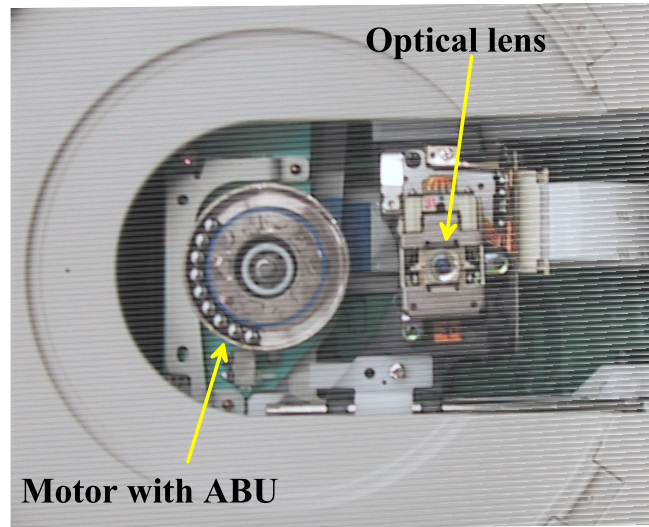


Figure 3: Example of an Automatic Balancing Unit, mounted in the GDR-8160B DVD-ROM Drive of LG Electronics. The CD or DVD is placed on top of the ABU by means of a magnetic coupling (not shown in the picture).

ABU consist of a rim with a number of balls, which will - in a certain range of rotating frequencies of the motor - be positioned such that the unbalance, due to deficiency in the axi-symmetry of the inertia properties of the CD disc, is counteracted. Other systems in which auto-balancing units are used are washing machines and hand-held tools. In the latter applications a viscous fluid is present in the ABU, ensuring that only viscous friction forces are present. The resulting dissipative forces acting on the balls ensure the stability of the balancing (equilibrium) positions of the balls. However, in a CDROM-system the use of such fluids is highly undesirable, since leakage would destroy the optical system. Therefore, the dry friction between rim and balls induces the necessary dissipative force. The discontinuities present in this system are due to the dry friction phenomena mentioned above and the contact (impact) between the balls. For more information on the working principle of the automatic balancing unit see [7]. The balancing performance of the ABU can be seriously affected by the stiction behaviour related to the dry friction present in the system, because the stiction phenomena leads to the existence of equilibrium *sets*. In other words, the balls can come to a standstill in a whole range of positions, which do not necessarily lead to balancing. So, the main research question is related to the assessment of the performance of a automatic balancing unit with dry friction.

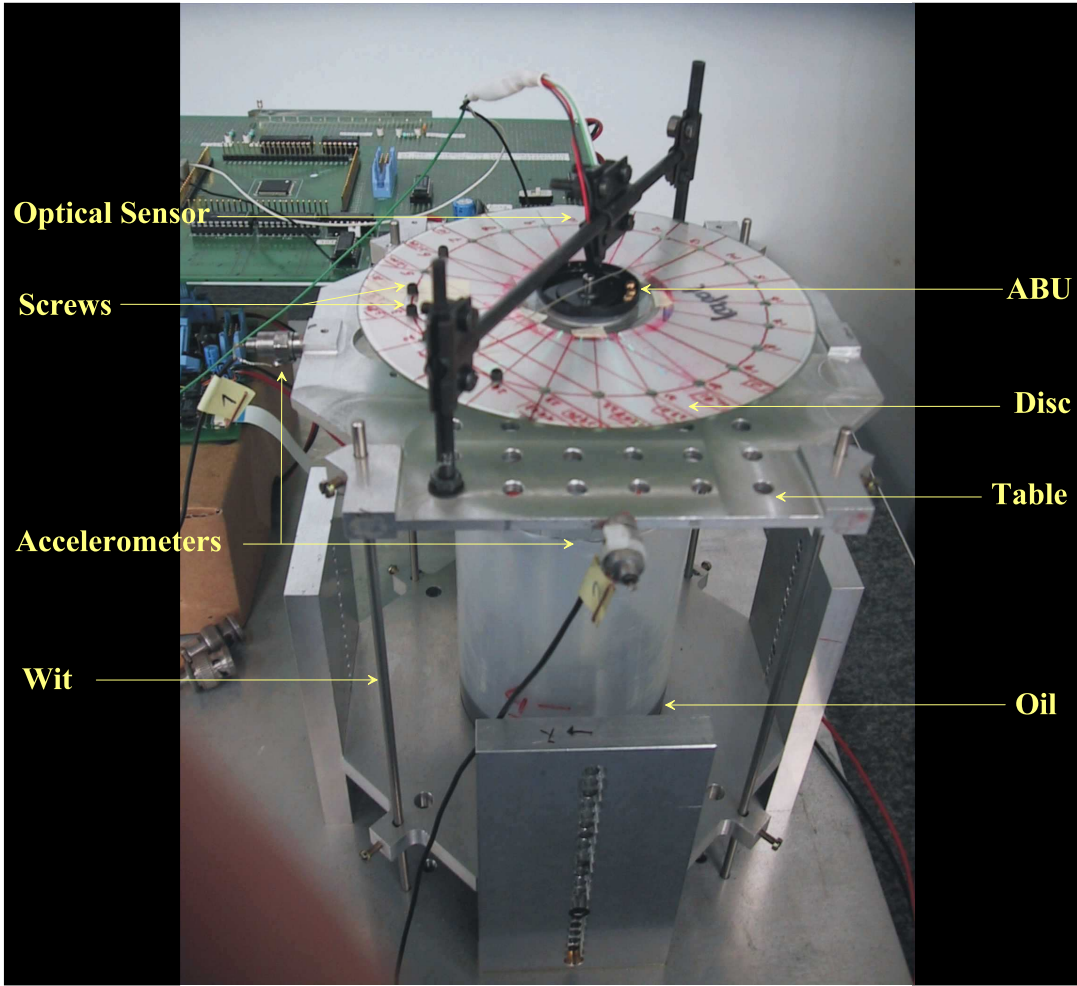


Figure 4: Picture of the experimental setup.

2.2 The experimental auto-balancing system

In the laboratory of the dynamics and control group of the Mechanical Engineering department of the Eindhoven University of Technology, an experimental setup incorporating an ABU in a CDROM system is available, see figure 4. This setup was originally designed and built at Philips Optical Storage, Eindhoven, The Netherlands. In this experimental system only two balls are present. A schematic representation of the experimental set-up is depicted in figure 5. Herein, it is assumed that all movements are in the horizontal plane and that the table does not rotate. The ABU consists of a table that is suspended by 4 wits. These can be modelled by two linear springs and dampers, positioned perpendicular to each other (stiffness parameters k_1 and k_2 and damping parameters b_1 and b_2), attached on the one end to the table, on the other end to inertial space. The motor that drives the ABU is attached to the table. The ABU is rigidly attached to the rotor part of the motor via the motor shaft, which drives the CD with a known angular velocity $\Omega(t)$. The total mass of the table, motor, ABU (without the balls) and the CD (without the imbalance) is called M_T . The imbalance mass in point C is m_I . The distance from the geometrical center of the ABU (point B in figure 5) to the imbalance (point C) is called e . The ABU contains two balls, each having mass m_i , $i = 1, 2$. These balls are free to move along the rim of the ABU. It is assumed that, under the influence of centrifugal forces, the balls are always in contact with the rim. The distance from the geometrical center of the ABU to the center of ball i is called l_i . Between

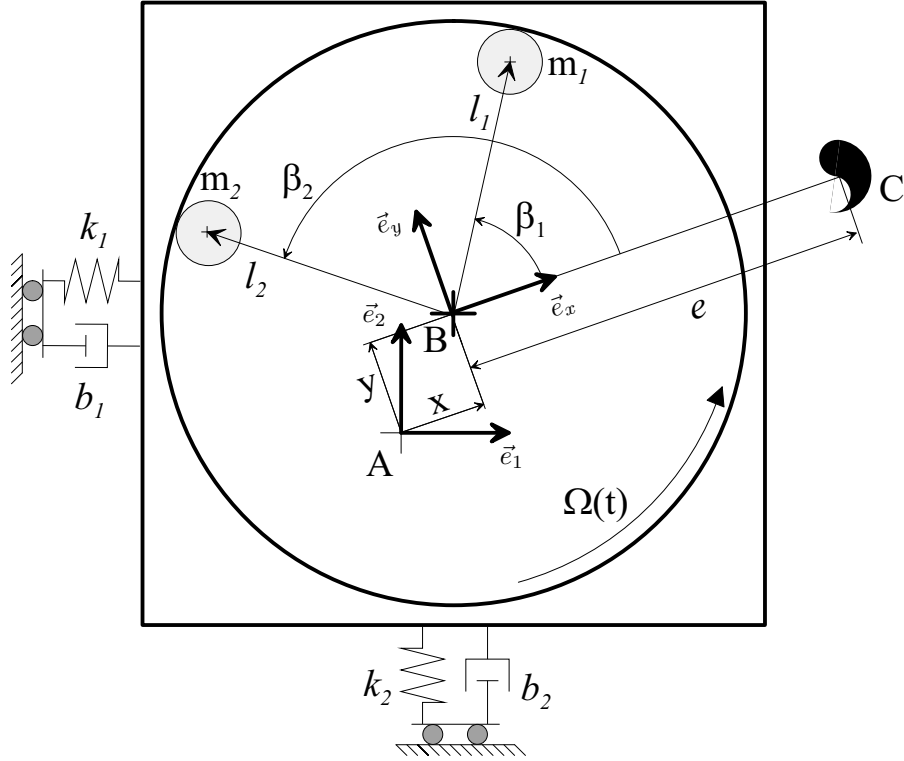


Figure 5: Schematic representation of the Auto Balancing Unit.

the balls and the rim, friction (rolling friction) is present, resulting in friction forces in tangential direction. It should be noted that in the current model contact between the balls is not modelled.

A model of the experimental system was built (see [7]) and can be formulated in terms of the generalized coordinates $\underline{q} = [x \ y \ \beta_1 \ \beta_2 \ l_1 \ l_2]^T$; see figure 5 for the definition of these coordinates. The model is formulated by:

$$\underline{M}(\underline{q})\ddot{\underline{q}} - \underline{h}(\underline{q}, \dot{\underline{q}}) = \underline{W}_T \lambda_T + \underline{W}_N \lambda_N, \quad (4)$$

where

$$\underline{M}(\underline{q}) = \begin{bmatrix} M & 0 & -m_1 l_1 \sin \beta_1 & -m_2 l_2 \sin \beta_2 & m_1 \cos \beta_1 & m_2 \cos \beta_2 \\ 0 & M & m_1 l_1 \cos \beta_1 & m_2 l_2 \cos \beta_2 & m_1 \sin \beta_1 & m_2 \sin \beta_2 \\ -m_1 l_1 \sin \beta_1 & m_1 l_1 \cos \beta_1 & m_1 l_1^2 + J_1 \left(\frac{2l_1}{d_1}\right)^2 & 0 & 0 & 0 \\ -m_2 l_2 \sin \beta_2 & m_2 l_2 \cos \beta_2 & 0 & m_2 l_2^2 + J_2 \left(\frac{2l_2}{d_2}\right)^2 & 0 & 0 \\ m_1 \cos \beta_1 & m_1 \sin \beta_1 & 0 & 0 & m_1 & 0 \\ m_2 \cos \beta_2 & m_2 \sin \beta_2 & 0 & 0 & 0 & m_2 \end{bmatrix},$$

$$\underline{W}_T = \begin{bmatrix} 0 & 0 \\ 0 & 0 \\ 1 & 0 \\ 0 & 1 \\ 0 & 0 \\ 0 & 0 \end{bmatrix}, \quad \underline{W}_N = \begin{bmatrix} 0 & 0 \\ 0 & 0 \\ 0 & 0 \\ 0 & 0 \\ -1 & 0 \\ 0 & -1 \end{bmatrix},$$

$$\underline{h}(\underline{q}, \dot{\underline{q}}) = [h_x \quad h_y \quad h_{\beta_1} \quad h_{\beta_2} \quad h_{l_1} \quad h_{l_2}]^T, \text{ with:}$$

$$\begin{aligned} h_x &= - \left\{ -2M\omega\dot{y} - M\omega^2x - m_I e\omega^2 - \right. \\ &\quad \left. (m_1l_1 \cos \beta_1 (\dot{\beta}_1 + \omega)^2 + m_2l_2 \cos \beta_2 (\dot{\beta}_2 + \omega)^2) + kx + b(\dot{x} - \omega y) \right\}, \\ h_y &= - \left\{ 2M\omega\dot{x} - M\omega^2y - \right. \\ &\quad \left. (m_1l_1 \sin \beta_1 (\dot{\beta}_1 + \omega)^2 + m_2l_2 \sin \beta_2 (\dot{\beta}_2 + \omega)^2) + ky + b(\dot{y} + \omega x) \right\}, \\ h_{\beta_1} &= - \left\{ 2m_1l_1\omega\dot{x} \cos \beta_1 + 2m_1l_1\omega\dot{y} \sin \beta_1 + m_1l_1\omega^2x \sin \beta_1 - m_1l_1\omega^2y \cos \beta_1 \right\}, \\ h_{\beta_2} &= - \left\{ 2m_2l_2\omega\dot{x} \cos \beta_2 + 2m_2l_2\omega\dot{y} \sin \beta_2 + m_2l_2\omega^2x \sin \beta_2 - m_2l_2\omega^2y \cos \beta_2 \right\}, \\ h_{l_1} &= - \left\{ 2m_1\omega \sin \beta_1 \dot{x} - 2m_1\omega \cos \beta_1 \dot{y} - m_1\omega^2 \cos \beta_1 x - m_1\omega^2 \sin \beta_1 y \right. \\ &\quad \left. - m_1l_1(\dot{\beta}_1 + \omega)^2 - \frac{2J_1}{d_1} \left(\frac{2l_1}{d_1} \dot{\beta}_1 - \omega \right) \dot{\beta}_1 \right\}, \\ h_{l_2} &= - \left\{ 2m_2\omega \sin \beta_2 \dot{x} - 2m_2\omega \cos \beta_2 \dot{y} - m_2\omega^2 \cos \beta_2 x - m_2\omega^2 \sin \beta_2 y \right. \\ &\quad \left. - m_2l_2(\dot{\beta}_2 + \omega)^2 - \frac{2J_2}{d_2} \left(\frac{2l_2}{d_2} \dot{\beta}_2 - \omega \right) \dot{\beta}_2 \right\}, \end{aligned}$$

where: $M = M_t + m_I + m_1 + m_2$. Moreover, $\underline{\lambda}_N = [F_{N_1} \quad F_{N_2}]^T$ is a column of Lagrange multipliers related to the normal forces between the balls and the rim of the auto-balancing unit (F_{N_i} is the normal force between ball i and the rim) and $\underline{\lambda}_T = [F_{T_1} \quad F_{T_2}]^T$ is a column of Lagrange multipliers related to the friction forces between the balls and the rim of the auto-balancing unit (F_{T_i} is the friction force between ball i and the rim). Moreover, the friction forces are modelled using a set-valued force law in order to account for the stiction behaviour which is observed in the experiments:

$$F_{T_i} \in -\mu_i |F_{N_i}| \text{Sign}(\dot{\beta}_i), \quad i = 1, 2. \quad (5)$$

Herein, $\text{Sign}(x)$ is the set-valued sign-function

$$\text{Sign}(x) = \begin{cases} \{-1\} & x < 0 \\ [-1, 1] & x = 0, \\ \{1\} & x > 0 \end{cases}, \quad (6)$$

and μ_i is the friction coefficient related to the contact between ball i and the rim. It should be noted that now the model, described by (4) and (5) is formulated as a differential inclusion.

2.3 Research questions

The following research questions are currently addressed and/or will be addressed in the future:

- Friction modelling;
- Determination of equilibrium sets and the related stability properties;
- Limit cycling;
- Experimental validation of the previous topics;
- Modelling of the contact and impact between the balls;
- Bifurcation analysis of equilibrium sets and branches of periodic solutions;

3 An Experimental Setup for Investigation of Friction-Induced Dynamics in a Positioning Control System

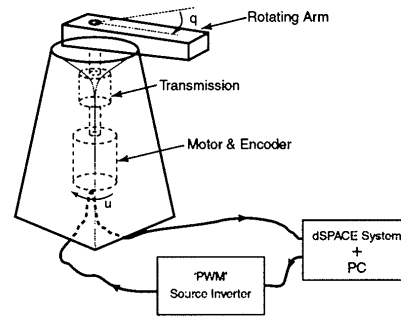
Devi Putra, Henk Nijmeijer and Nathan van de Wouw
Eindhoven University of Technology
Department of Mechanical Engineering
Dynamics and Control Group

3.1 Introduction

Friction occurs in many mechanical systems, e.g. bearings, servo systems, and robotic manipulators [8; 9; 10]. In positioning control systems, friction can severely deteriorate systems performance in terms of tracking errors, large steady-state errors, and limit cycling oscillations. It is, therefore, important to understand friction phenomena and their effect on the systems performance. The availability of precise experimental observations has been a good driving force for investigations of friction models and compensation techniques of friction [8; 9; 11; 10]. Since friction is a highly nonlinear phenomenon, it is very difficult to derive a complete friction model. Thus, a good matching between experimental observations and theoretical results is an important aspect in studying friction-induced phenomena.



(a) Picture of the setup



(b) Schematic diagram of the rotating arm system

Figure 6: The rotating arm inverted pendulum setup

3.2 The Rotating Arm Inverted Pendulum Setup

The experimental setup is a rotating arm manipulator with an inverted pendulum attached to the arm as shown in Figure 6(a). The rotating arm system consists of an induction motor, a planetary transmission, and a rotating arm as depicted in Figure 6(b). Due to bearings and seals in the motor and in the transmission, the inertia of the total system, i.e. the combined inertia of the separate elements, is subject to friction. The system is controlled using a PC with a dSPACETM system [12] and SimulinkTM. The angular displacement of the rotating arm is measured using a rotational encoder. Currently, we consider only the rotating arm system without the inverted pendulum.

The rotating arm system can be considered as a block mass that is moved by an input torque on a non-smooth surface. Its dynamics is described by a second-order differential equation

$$\dot{x} = Ax - Bf(x, u) + Bu \quad (7)$$

$$y = Cx \quad (8)$$

where $x = [x_1 \ x_2]^T$ is the state with x_1 and x_2 the position and the velocity of the block, respectively, $A = \begin{bmatrix} 0 & 1 \\ 0 & -D/J \end{bmatrix}$, $B = \begin{bmatrix} 0 \\ 1/J \end{bmatrix}$ with D the damping coefficient of the viscous friction, f is the nonlinear friction force, u is the input torque, $C = [1 \ 0]$, and y is the measured position. It should be noted that the friction is modelled by a set-valued force law (the stiction phenomena is important in the behaviour of the setup). Consequently, (7) forms a differential inclusion.

3.3 Research Topics

The rotating arm setup is used to study friction induced dynamics in positioning control systems. The problems that have been addressed are:

- a. Friction dynamics and parameter identification in pre-sliding regime, see [13].
- b. Stick-slip limit cycling in PID control system, see [14].
- c. Investigation of friction models and parameter identification of the models, see [15; 16].
- d. Designing of high performance regulator control for systems with friction, see [17].
- e. Limit cycling and bifurcation of limit cycles in observer-based controlled systems with friction, see [18; 16].
- f. Stability analysis and limit cycling phenomenon of reduced-order observer-based controlled systems with friction.

3.4 Open Problems

There are some problems emerge from the current research, namely:

- a. Stability analysis of equilibrium sets in positioning control systems.
- b. Design procedures for controller and observer, which guarantee that the closed loop system does not exhibit limit cycling.

4 Piece-Wise Linear Beam System

Apostolos Doris, Nathan van de Wouw and Henk Nijmeijer
 Eindhoven University of Technology
 Department of Mechanical Engineering
 Dynamics and Control Group

4.1 Introduction

The piece-wise linear beam system consist of a steel beam, which is clamped on two sides and supported at a discrete location by a one-sided linear spring. Moreover, the beam is excited by a force F . The supported beam system can be modelled by a piece-wise linear system, see section 4.2. In Figure 7, the beam system is depicted schematically. The piece wise linear beam system can serve as benchmark system for many piece-wise linear

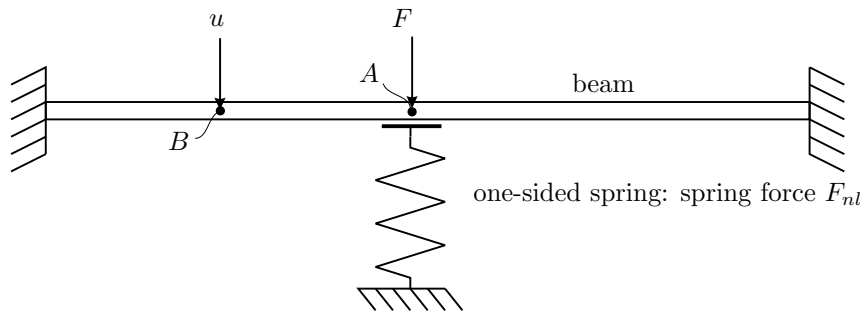


Figure 7: The piece-wise linear beam system.

systems in engineering practice. This will be advocated by three examples originating from different disciplines within the engineering practice; namely; suspension bridges, gearboxes, and atomic force microscopes.

Suspension bridges, such as the collapsed Tacoma Narrows bridge or the Golden Gate bridge, consist of a large roadbed, which is supported at both ends by a bridge tower; see the left part of Figure 8. Some bridges have two suspension cables between these towers whereas intermediate vertical hangers are placed at discrete positions along the roadbed and the suspension cables. Other bridges have a number of suspension cables between the towers and discrete positions along the roadbed. Suspension bridges excited by wind or earthquakes sometimes show large amplitude vertical vibrations of the roadbed, which can cause the bridge to collapse. These vibrations cannot be explained by resonance phenomena known from linear dynamics. Therefore, many authors have proposed nonlinear dynamical models. These models possess characteristics similar to the piece-wise linear beam system, namely: a roadbed modelled as a beam supported at both ends, the suspension cables (and hanger) modelled by one-sided springs, see the right part of Figure 8, and the excitation of the bridge towers by wind modelled as a harmonic force applied to the beam.

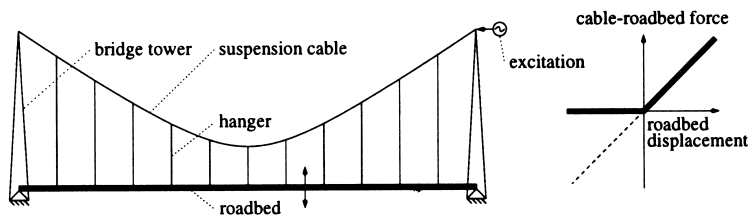


Figure 8: Suspension bridge model based on [19].

Gearboxes play a major role in the transmissions of machines and automobiles; see the left part of Figure 9. They are known to possess rattling, which causes noise in machines and decreases comfort of automobiles. Rattling is caused, among other things, by the inevitable backlash in the meshes of the gears. Backlash in the gears is often modelled with piecewise linear spring forces, see the right part of Figure 9 whereas the gears themselves are modelled by single-degree-of-freedom or multi-degree-of-freedom linear models. Gearboxes are excited by a drive train system that contains torsional vibrations generated by imbalances of the engine. These vibrations can be modelled by periodic excitations. The use of linear models combined with piece-wise linear spring forces (subjected to periodic excitations) reflects the similarity with the piece-wise linear beam system.

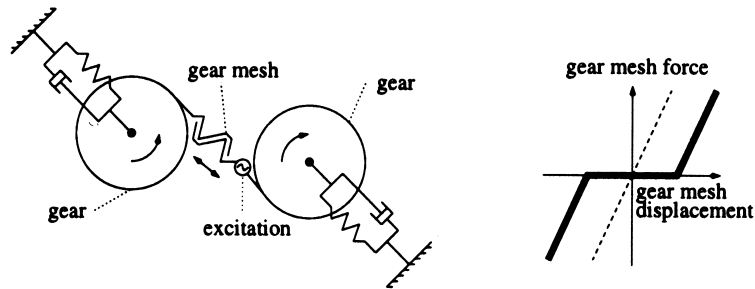


Figure 9: Gearbox model based on [20].

Atomic force microscopes are used to obtain nanometer scale images of surfaces on a wide variety of materials; see the left part of Figure 10. The microscope consists of a clamped beam -often made of aluminium foil- with a stiff tip attached to its free end. This tip is allowed to impact on the sample after exciting the beam or the sample harmonically. An external excitation is applied to prevent the sample from being damaged, which would occur when scanning the surface under constant load. The deflections of the beam measured at the tip provide the topographic information on the surface of the sample. When scanning soft materials such as polymers or biological materials, the stiffness variation between contact and non-contact at the tip can be modelled by a piecewise linear spring force; see the right part of Figure 10. This results in a model similar to the beam system.

The previous examples demonstrate the practical relevance of studying a piece-wise linear beam system. Besides, it is worth mentioning that they cover a wide range from small-scale to large-scale systems within engineering practice.

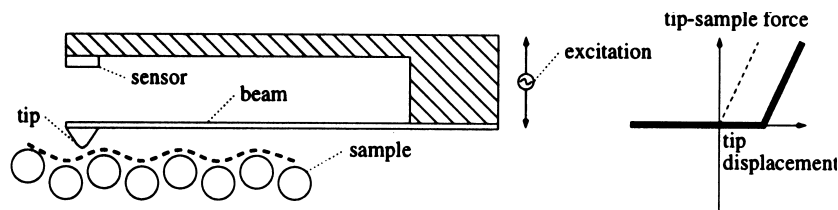


Figure 10: Atomic force microscope model based on [21].

4.2 Problem Formulation

4.2.1 Experimental Setup

A schematic view of the lab-scale setup of the piece-wise linear beam system is depicted in Figure 4.2.1. Figure 4.2.1 depicts a photo view of the setup. The beam system is excited by a rotating mass-unbalance that generates a harmonic force F at the middle of the beam (point B in Figure 7). A tachometer-controlled motor that enables a constant rotation speed drives the mass-unbalance. For positive displacements of the middle of the beam, a second beam which is clamped at both ends and which represents the one-sided spring generates a restoring force F_{nl} . At point A , a control force u can be applied. The control force is generated by a shaker-amplifier combination. Transversal displacements of the beam are measured at two points using linear variable differential transformers LVDTs: at point A (q_{mid}) and at point B (q_{act}). Moreover, at these points accelerations are measured using piezoelectric accelerometers and piezoelectric force transducers measure the forces F and u . The computation of the control force and the data processing and acquisition of the measurements are performed with the real-time software/hardware environment dSPACE combined with MATLAB's Simulink.

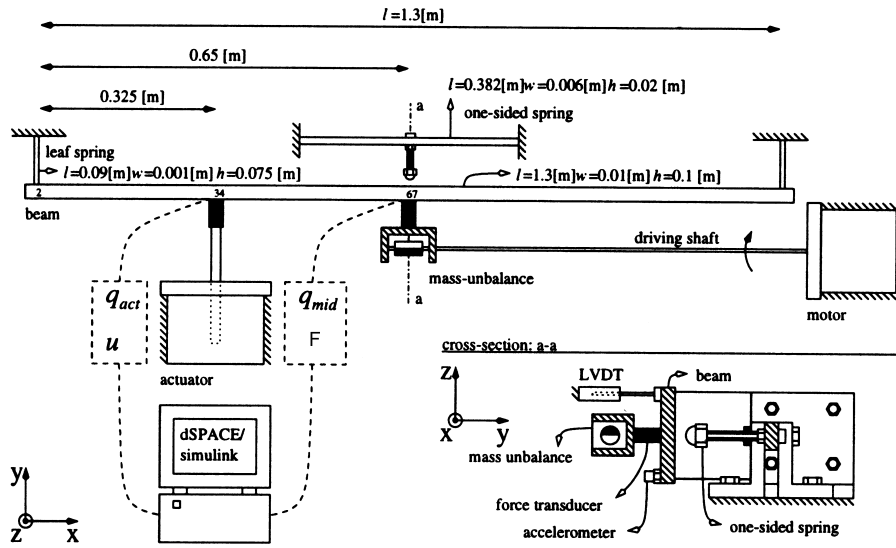


Figure 11: Schematic description of the experimental setup [22].

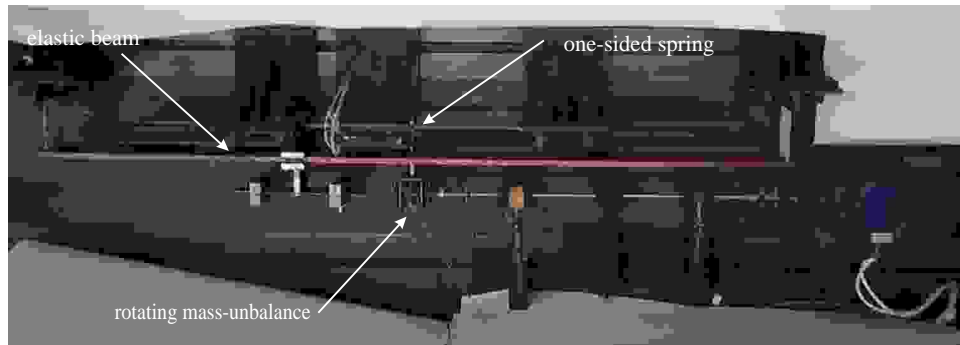


Figure 12: Photo of the experimental setup.

4.2.2 Model of the piece-wise linear beam system

The schematic representation of the piece-wise linear beam system is depicted in Figure 7. The system consists of a beam with uniform cross section supported at both ends. A periodic excitation force F is applied at the middle of the beam. Only when the middle of the beam moves downwards from its equilibrium position, a restoring force F_{nl} caused by the one-sided spring is acting on the beam. As this force originates from a linear (though one-sided) spring, two linear regimes can be distinguished based upon the position of the middle of the beam: one regime determined by the stiffness of the beam only and one regime determined by the combined stiffness of the beam and the one-sided spring in parallel. Thus, the supported beam is a piece-wise linear system.

A simple, though sufficiently accurate, three-degree-of-freedom model (3-DOFs) of the beam will be used for the piece-wise linear beam system. This model is obtained by reducing a sophisticated finite element model (of the elastic beam without one-sided support) with 105-degree-of-freedom through application of a component mode synthesis method [22]. This reduction is applied to reduce the computational effort to analyse the dynamic behaviour of the beam system and simplify controller and observer design. The 3-DOF model is formulated in terms of three generalized coordinates: $\underline{q} = [q_{act} \ q_{mid} \ q_{\xi}]^T$. As mentioned above, q_{act} and q_{mid} represent displacements at the points B and A , respectively. Furthermore, the third generalized coordinate q_{ξ} accounts for the first free-interface eigenmode of the beam. The location of point A is fixed at the middle of the beam whereas the location of point B can be defined between the left clamp and the middle of the beam. The equation of motion for the 3-DOF model of the piece-wise linear beam system can be written as

$$\underline{M}\ddot{\underline{q}} + \underline{B}\dot{\underline{q}} + \underline{K}\underline{q} + \underline{F}_{nl}(\underline{q}) = \underline{h}_2 F + \underline{h}_1 u,$$

where \underline{M} , \underline{B} and \underline{K} are the mass matrix, damping matrix and stiffness matrix, respectively, and the restoring force of the one-sided spring \underline{F}_{nl} is given by

$$\underline{F}_{nl}(\underline{q}) = k_{nl} \epsilon(q_{mid}) \underline{h}_2 \underline{h}_2^T \underline{q} \quad \text{with} \quad \epsilon(q_{mid}) = \begin{cases} 1 & q_{mid} > 0 \\ 0 & q_{mid} \leq 0 \end{cases}.$$

The force $F = F(t)$ represents an external excitation applied to the beam system, for example a harmonic force. Furthermore, \underline{h}_i , $i = 1, 2$, is defined as the i -th column of the identity matrix and k_{nl} is the stiffness of the one-sided spring.

4.3 Research Problems

The following research problems with respect to the piece-wise linear beam system will be addressed:

- Observer design for the piece-wise linear beam system. An observer is needed to support the implementation of a state-feedback controller. Here we will use observer design techniques as described in [23];
- Experimental assessment of the performance of the observer design;
- Controller design for piece-wise linear systems such as the beam with one-sided support.

References

- [1] Brett, J. F. The genesis of torsional drillstring vibrations. *SPE Drilling Engineering* , (1992), 168–174.
- [2] Kust, O. *Selbsterregte Drehschwingungen in schlanken Torsionssträngen: Nichtlineare Dynamik und Regelung*. Ph.D. thesis, Technical University Hamburg-Harburg, 1997.
- [3] Jansen, J. D. *Nonlinear Dynamics of Oil-well Drill-strings*. Ph.D. thesis, Delft University of Technology, 1993.
- [4] Leine, R. *Bifurcations in Discontinuous Mechanical Systems of Filippov-Type*. Ph.D. thesis, Eindhoven University of Technology, 2000.
- [5] van den Steen, L. *Suppressing Stick-Slip-Induced Drill-string Oscillations: a Hyper Stability Approach*. Ph.D. thesis, University of Twente, 1997.
- [6] N. Mihajlovic, A. A. van Veggel, N. v. d. W. H. N. Analysis of friction-induced limit cycling in an experimental drill-string system. *ASME Journal of Dynamic Systems, Measurements and Control* .
- [7] Heuvel, v. d. M. *Modeling and Analysis of an Automatic Balancing Unit*. Master’s thesis, Eindhoven University of Technology, The Netherlands, 2002.
- [8] Armstrong-Hélouvry, B., Dupont, P. and de Wit, C. C. A survey of models, analysis tools, and compensation methods for the control of machines with friction. *Automatica* **30**, (1994), 1083–1138.
- [9] Armstrong-Hélouvry, B. *Control of Machines with Friction*. Kluwer Academic Publishers, 1991.
- [10] Olsson, H., Åström, K. J., de Wit, C. C., Gäfvert, M. and Lischinsky, P. Friction models and friction compensations. *European Journal of Control* **4**, (1998), 176–195.
- [11] de Wit, C. C., Olsson, H., Åström, K. J. and Lischinsky, P. A new model for control of systems with friction. *IEEE Transaction on Automatic Control* **40**, (1995), 419–425.
- [12] dSPACE. *DS1102 User’s Guide*. dSPACE digital signal processing and control engineering GmbH, 1999.
- [13] Hensen, R., van de Molengraft, M. and Steinbuch, M. Frequency domain identification of dynamic friction model parameters. *IEEE Transactions on Control Systems Technology* **10**, (2002), 191–196.
- [14] Hensen, R. and van de Molengraft, M. Friction induced hunting limit cycles: an event mapping approach. In *Proceeding of the American Control Conference 2002*. Anchorage, AK, 2002.
- [15] Hensen, R. H. A. *Controlled Mechanical Systems with Friction*. Ph.D. thesis, Eindhoven University of Technology, The Netherlands, 2002.
- [16] Putra, D. and Nijmeijer, H. Limit cycling in an observer-based controlled system with friction: Numerical analysis and experimental validation. *submitted to International Journal of Bifurcation and Chaos* .
- [17] Hensen, R., van de Molengraft, M. and Steinbuch, M. High performance regulator control for mechanical systems subjected to friction. In *Proceedings of the 2001 IEEE International Conference on Control Applications*. Mexico City, 2001.
- [18] Putra, D. and Nijmeijer, H. Limit cycling in observer-based controlled mechanical systems with friction. In *Proceedings of the 2003 European Control Conference (to appear)*. Cambridge, 2003.
- [19] Briyja, D. and Śniady, P. Stochastic nonlinear vibrations of highway suspension bridges. *Journal of Sound and Vibration* **216**(3), (1998), 507–519.
- [20] Karagiannis, K. and Pfeiffer, F. Theoretical and experimental investigations of gear-rattling. *Nonlinear Dynamics* **2**, (1991), 367–387.

- [21] Hansma, P., Elings, V., Marti, O. and Bracker, C. Scanning tunneling microscopy and atomic force microscopy: application to biology and technology. *Science* **242**, (1988), 209–216.
- [22] Heertjes, M. *Controlled Stabilization of Long-Term Solutions in a Piece-wise Linear Beam System*. Ph.D. thesis, Eindhoven University of Technology, 1999.
- [23] Juloski, A., Heemels, W. and Weiland, S. Observer design for a class of piece-wise affine systems. In *Proceedings of the 41st IEEE Conference on Decision and Control, Las Vegas, Nevada, USA*.